Corrosion, Mechanical and Wear Properties of nano-ZnO doped Aluminium

K.S. Harishanand[1], H. Nagabhushana[2], B.M. Nagabhushana[3], Parimesh Panda [1], A H Adarsha[1], M.M. Benal[4], N Raghavendra[1], K R Vishnu Mahesh[5]

[1](Department of Mechanical Engineering, R.V. College of Engineering, Bengaluru-560059, India)
[2](Department of Physics, Tumkur University, Tumkur-572103, India)
[3](Department of Chemistry, M.S. Ramaiah Institute of Technology, Bengaluru-560054, India)
[4](Department of Mechanical Engineering, Govt. Engineering College, Kushalnagar-571234, India)
[5](Department of Chemistry, ACS College of Engineering, Bengaluru-560074, India)

ABSTRACT

Zinc Oxide (ZnO) Nano powder was produced by Solution Combustion Synthesis (SCS) at $350 \pm 10°$ C temperature using sugar solution as fuel. The final product was characterized by means of XRD, SEM and EDX. The powder blends of ZnO/Al were prepared by low energy ball milling and the composite blocks of ZnO/Al were fabricated by powder metallurgy technique. The microhardness, wear resistance and corrosion resistance of ZnO/Al blocks were studied. The results show that the microhardness, wear resistance and corrosion resistance can be improved significantly with addition of ZnO nano powder up to 1 wt%; at the same time, the optimal microhardness and microstructure were obtained when the mass fraction of ZnO nano powder is 1wt% where as sample with 5 wt% of ZnO nano powder show best wear resistance. Corrosion tests reveal that there was a slight mass loss due to corrosion.

Keywords – ZnO, Microhardness, Wear resistance, Corrosion resistance and Microstructure.

1. INTRODUCTION

Aluminium and its alloys are widely used in services such as transportation, armory and marine industries due to their high strength to weight ratio. They relatively resist corrosion when exposed to various aggressive environments. These environments may include water vapour, acid and base solutions. Most of these environments degrade the quality of Aluminium and its alloys and affects the mechanical properties of the system thereby reducing their life-span. This makes them unstable in certain environment that enhances their chemical combination with other elements in the environment to form stable compounds. On the return to their natural stable form of ground state known as ores an accompanying reduction in the free energy of the system occurs. These structural defects could be a major determinant in the degree of resistance of metal components to the effects of media-driven corrosion [1-3].

Superior properties of metal oxides such as refractoriness, high hardness, high compressive strength, wear resistance etc. make them suitable for being used as reinforcement material in metal matrix. Incorporating ultra-fine particles of metal-oxides significantly improves mechanical properties of the metal matrix by reducing the inter-particle spacing and providing their inherent properties to the metal matrix since they get embedded uniformly into it. However, fine particles show higher tendency towards agglomeration. Therefore, optimum particle size, amount of reinforcement and processing parameters (compaction pressure, sintering temperature, sintering time) should be determined for each technique and matrix. Nano-particles represent appropriate wettability with metal at the time of sintering and good stability as well [4-8].

ZnO metal oxide plays a very important role in many areas of chemistry, physics, and material science. In technological applications, ZnO is used in the fabrication of microelectronic circuits, sensors, piezoelectric devices, fuel cells, coatings for the passivation of surfaces against corrosion. The nanometric field is governed by numerous surface phenomena (photosynthesis, catalysis, precipitation, reactivity, deformation, reflectivity, luminosity). This is so because in nanomaterials the number of atoms which are localized on free surfaces as well as on internal interfaces may be equal or higher than the number of atoms localized inside the grains. On this account, the properties are strongly influenced by the interfaces present (surfaces, grain boundaries) [9-13].

Among the functional mineral compounds such as Perovskite ($CaTiO_3$), Rutile (TiO_2), CaF_2, Spinel ($MgAl_2O_4$), Wurtzite (ZnS) and Zincite (ZnO), the last one being unique because of its dual

semiconducting and piezoelectric properties. Due to the combination of interesting piezoelectric, electric, optical and thermal properties, ZnO-doped nanomaterials are of high interest for multifunctional applications in gas sensors, ultrasonic oscillators or transparent electrodes in solar cells [14-18].

Nanostructured ZnO is a material that may present various structures, whose configurations are much richer than for any known nanomaterial including carbon nanotubes. The n-type conductivity of ZnO is relatively easy to be obtained by using Zn in excess or by doping ZnO with Al, Ga, In. The most promising dopants for obtaining p-type conductivity are the elements from the Vth group. Different routes to obtain doped ZnO that have been studied yet are : the incorporation of transition metal ions into a semiconductor photo catalyst by ion implantation or by co-precipitation; introduction of oxygen vacancies by treating a photo catalyst with hydrogen plasma or X-ray irradiation; coupling semiconductors (ZnO or TiO_2) with oxides or sulfides that enable visible light absorption (WO_3, Fe_2O_3, CdS) by co-precipitation or impregnation; doping of N-atoms into the substitution sites in the crystal structure of a photo catalyst. In the science and technology of ZnO, several key issues that have to be achieved includes controlling the morphology and chemical composition of the ZnO powders, controlling the purity and particle size during the synthesis process of ZnO powders, controlling the amount of the dopants. ZnO powders with different morphology (prismatic, ellipsoidal, bi-pyramidal, dumbbell-like, nanowire, nanorod) have been obtained till date [18-23].

Different physical or chemical synthetic approaches have been developed to produce nano-sized ZnO particles including thermal decomposition, thermolysis, chemical vapor deposition, sol–gel, spray pyrolysis, precipitation vapor phase oxidation, thermal vapor transport, condensation and hydrothermal. Generally, these preparation methods involve complex procedures, sophisticated equipment and rigorous experimental conditions. Most of these techniques require high temperatures and long processing time. Indeed, there is great demand for economically viable synthesis techniques. Solution Combustion Synthesis (SCS) is emerging as a promising technique for the preparation of nanopowder. This process is simple, fast, economic and does not require high temperature furnaces and complicated lab set-ups. It can be used for the preparation of all kinds of oxides [23-28].

From the open literature [1-28], the ZnO based Aluminium composites attracted much attention in various applications, hence in this work, the nano-ZnO/Al powder blends were used to prepare ZnO/Al blocks by cold pressing followed by sintering and the performance of the fabricated blocks were studied for hardness, wear resistance and corrosion resistance.

2. EXPERIMENTAL
2.1. Synthesis of ZnO powder
The ZnO powder was prepared by dissolving Zinc Nitrate ($Zn(NO_3)_2.6H_2O$) and sugar solution in a minimum quantity of double distilled water in a Pyrex dish. The dish containing the solution was introduced into a pre-heated muffle furnace maintained at $350 \pm 10ºC$. The solution initially boils and undergoes dehydration followed by decomposition with the evolution of large amount of gases. At the point of spontaneous combustion, the solution begins burning and releases lot of heat. All the solution vaporizes instantly and becomes a burning solid. The entire combustion process for producing ZnO powder takes only 5 min. The formation of ZnO nano powder by combustion synthesis can be represented by following reaction:

$$Zn(NO_3)_2 + C_2H_6N_4O_2 \rightarrow ZnO + 3N_2 + 2CO + 3H_2O$$
…………………….. (1)
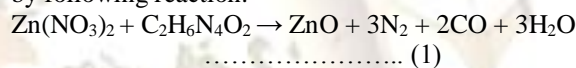
2.2. Preparation of ZnO/Al powder blends and ZnO/Al blocks
ZnO nano powder produced by Solution Combustion Synthesis(SCS) was added to 99.5% pure commercially available Aluminium powder with wt% of ZnO nano powder varying from 0 to 5% with an increment of 0.25, 0.5, 1, 2.5 and 5 wt%. They were mixed for 30 minutes by hand mixing and loaded in metal die for compaction. The powder metallurgy technique was used to fabricate the ZnO doped Al blocks. Powder blends were cold pressed at 200 MPa to approximately 90 % compression and then sintered at 500° C for 1 hour. The sintered ZnO/Al blocks were polished with fine emery papers with grit size ranging from 200 to 2000 followed by diamond paste polishing to obtain mirror finish surface on the specimen blocks.

2.3. XRD, Surface Morphology, EDX and Microstructures of ZnO and ZnO/Al blocks
X-ray Diffractometer (XRD: Shimandzu 700 S, Japan), Scanning Electron Microscopy (SEM: JEOL, Japan, JSM 840A) were employed to analyze the powder and morphology of the ZnO powder and polished surfaces of ZnO/Al blocks. The grain size and microstructure were studied by using optical microscope.

2.4. Micro-hardness test
Micro hardness was tested using Vickers Micro-hardness tester with diamond indenter in the

form of right pyramid and a square base. An optical microscope with up to 400X magnification along with a Micrometer attachment in the eye piece was used to observe and measure the length of the diagonal of indentation. Microscope attachment helps in determining the distribution of ZnO nano powder dopant in the Al matrix doped with varying percentages ranging from 0 to 5%.

2.5. Wear resistance test

Pin on disc apparatus was used to measure the wear resistance of the samples. ZnO/Al samples of size $10\times10\times20$ mm^3 were fabricated and mounted on Pin on disk apparatus and made to rub against the rotating stainless steel disk. Area exposed to wear was 10×10 mm^2. Relative velocity of wear test sample with respect to the rotating disk was 2.6 ms^{-1} and sliding distance was 1.57 km. Mass loss due to wear was calculated for each sample after completion of wear test.

2.6. Corrosion resistance test

Two separate tests were performed to evaluate the corrosion resistance of the ZnO/Al blocks.
2.6.1. The specimens were soaked in the spray tank with 3.5% NaCl solution for 50 hr and then were rinsed, dried and weighed. The corrosion resistance was evaluated by mass loss per area, $\Delta m/S$ (Δm is the mass loss and S is the surface area).
2.6.2. The specimens were soaked in the spray tank with 0.5 mol MgSO$_4$ solution for 10 hr and then were rinsed, dried and weighed.

3. RESULTS AND DISCUSSIONS
3. 1 X-Ray Diffractometer (XRD) Studies

The crystallinity and purity of the prepared product has been confirmed by powder X-ray diffraction. Fig.1 shows PXRD of ZnO nanoparticles which shows a well defined peaks located at Bragg angles (2θ) = 30º, 33º, 35º corresponding to planes having Miller Indices (100), (002), (101) respectively. The characteristic peaks are higher in intensity which indicates that the products are of good crystalline nature. No peaks corresponding to impurities are detected, showing that the final product is purely ZnO. It is observed that intensity of the peaks increases with thermal treatment due to agglomeration, which means that the crystallinity has been improved. The full width at half maxima of major peaks decreases and confirms the grain size growth [29].
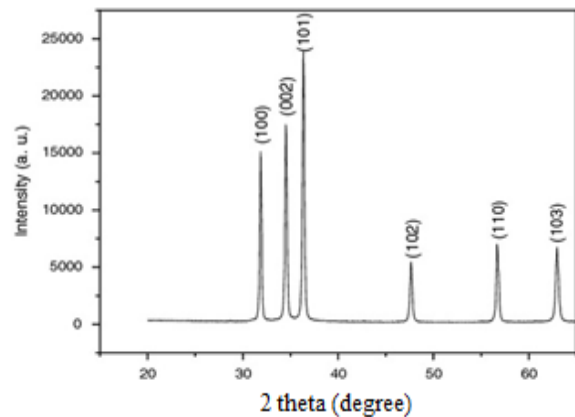

Figure.1 XRD Pattern of ZnO nano powder

3.2. Morphological study using SEM and Elemental composition using EDX

From the SEM analysis as shown in the Fig.2a, Fig.2b, Fig.2c, Fig.2d, Fig.2e, Fig.2f, it is observed that the circular shaped primary particles are agglomerated with varying sizes with aluminum powder. Here, the particle size was greatly dependent on the calcination temperature. As calcination temperature increases the size also increases, due to congregation effect, which is reflected in surface area and XRD measurements.

From the EDX Spectrum, it is clearly observed that no or relatively a small peak at 0.5 wt % ZnO doped aluminum composites sample and remarkably high peaks of ZnO presence at 5 wt % ZnO doped Aluminium composites sample is a clear indication shown in Fig.3a and Fig.3b. The spectrum reveals only the presence of Aluminium and ZnO elements and the absence of other elements as the spectrum exhibits the peaks for aluminum and ZnO only. Therefore, it can be stated that the physical and mechanical parameters can be attributed to the presence of above said two elements in the composition.
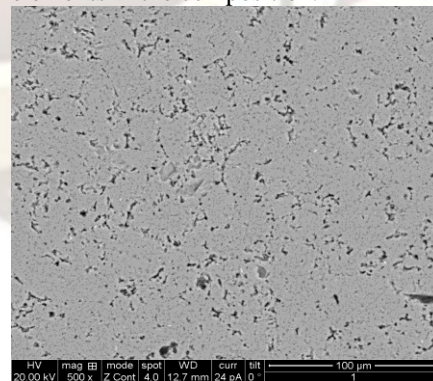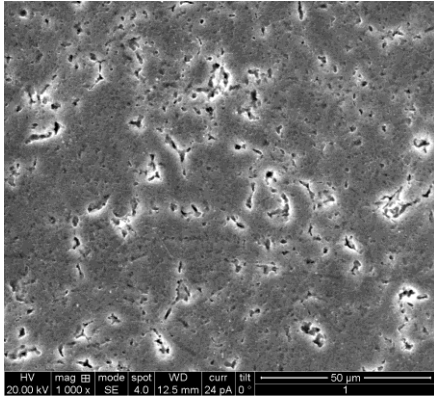

Figure.2a SEM Micrograph of Bare Aluminium

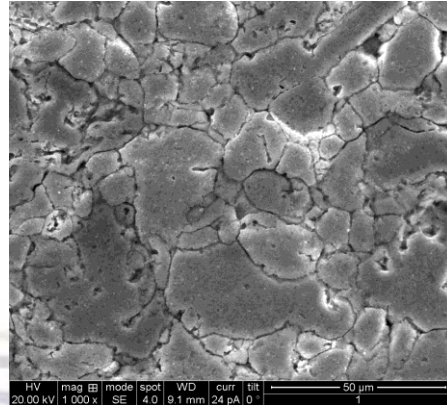**Figure.2b** SEM Micrograph of 0.25% ZnO doped Al

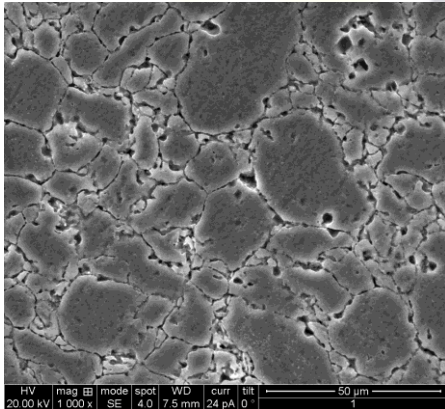**Figure.2f** SEM Micrograph of 5% ZnO doped Al

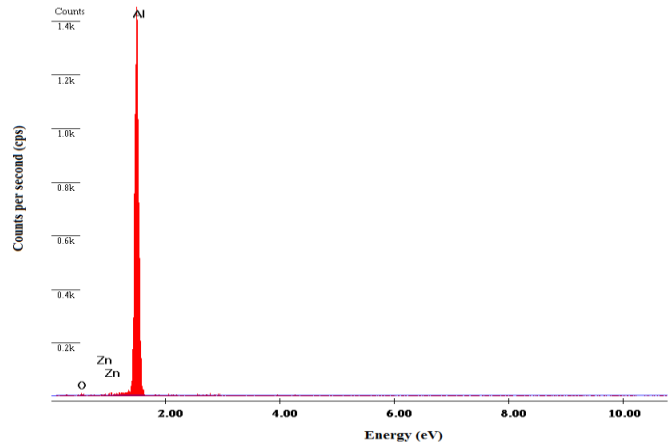**Figure.2c** SEM Micrograph of 0.5%ZnO doped Al
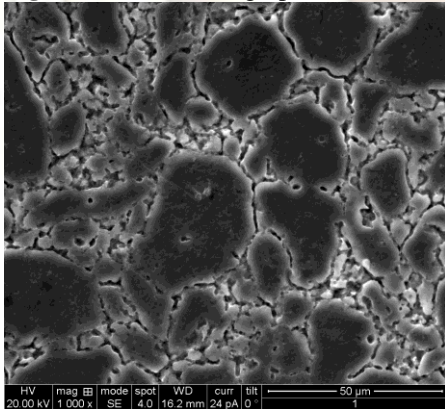

Figure.3a EDX of 0.25% doped ZnO/Al composite
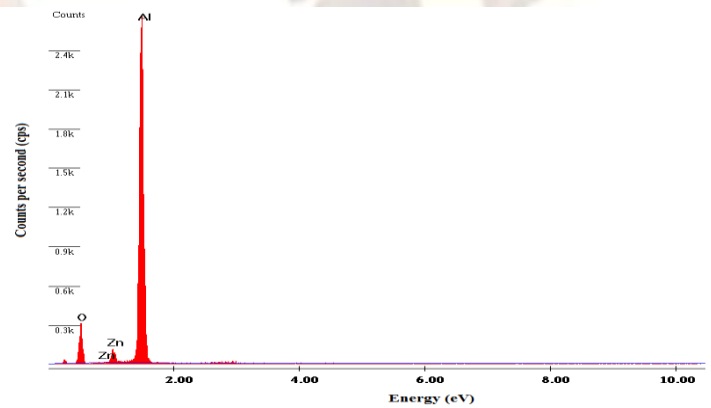

Figure.2d SEM Micrograph of 1% ZnO doped Al
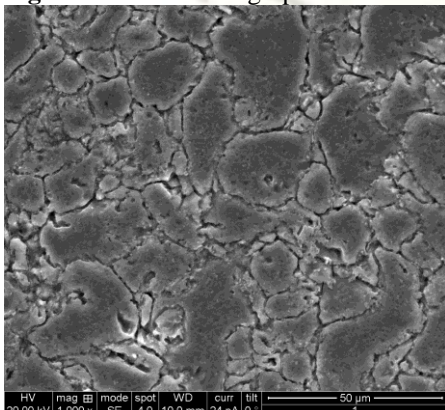

Figure.3b EDX of 5% doped ZnO/Al composite

3.3. Micro-hardness or Vickers hardness test

Hardness of a material is defined as the resistance to deformation, particularly permanent deformation, indentation or scratching. Vickers hardness value increased by 3.3, 9.09, 21.05, 18.91 and 9.09 % with the addition of 0.25, 0.5, 1, 2.5 and 5 wt% ZnO nano powder respectively in Aluminium matrix. Micro hardness of nano-ZnO doped Aluminium blocks increased with increase in

Figure.2e SEM Micrograph of 5% ZnO doped Al

percentage of ZnO up to 1 wt% and further no significant increase is observed. The microhardness graph shown in Figure4 clearly indicates a slow growth in hardness at lower wt% of nano-ZnO. A remarkable and substantial increment in hardness is observed at 1 wt% nano-ZnO concentration due to uniform distribution of nano-ZnO in the substrate.

With further addition of nano-ZnO, a decline in the hardness is observed which could be attributed to an uneven distribution of the nano-ZnO particles and their tendency to agglomerate at concentrations higher than 1 wt% of nano-ZnO. This means superior interfacial bond strength and related high value of hardness can be achieved at 1 wt% of nano-ZnO as the optimal value.
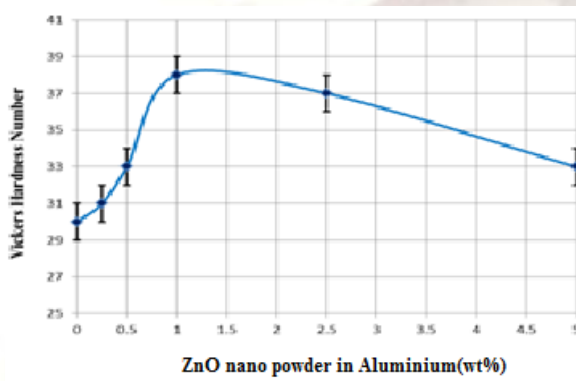

Figure.4 Variation of Wear Resistance with addition of nano-ZnO

3.4. Micro structure and Morphology analysis of sintered ZnO/Al blocks

The micro structure at different doping concentrations is shown in Fig.5a, Fig.5b, Fig.5c, Fig.5d. ZnO particles can be seen well embedded in the grains of Aluminium matrix shown as a result of which the structure becomes closer and grains compact. ZnO nano particles are uniformly distributed in Al matrix in case of lower wt% of ZnO powder up to 1 wt% and agglomeration of ZnO cannot be seen in major part of the Al matrix as shown. This reveals that the sample has uniform structure and steady performance at doping percentages less than 1%. At higher doping percentages (2.5% and 5%), agglomeration of ZnO is more common in the aluminium matrix and the ZnO particles are not evenly distributed as shown. This uneven distribution and agglomeration of ZnO in the Al matrix leads to density variations from one region of the matrix to another. The presence of nano particles in the grain boundaries was the cause for suppression of non-coulombic loss of the grains and hence self-corrosion.
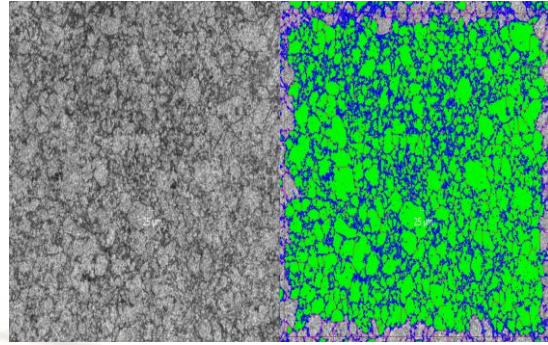

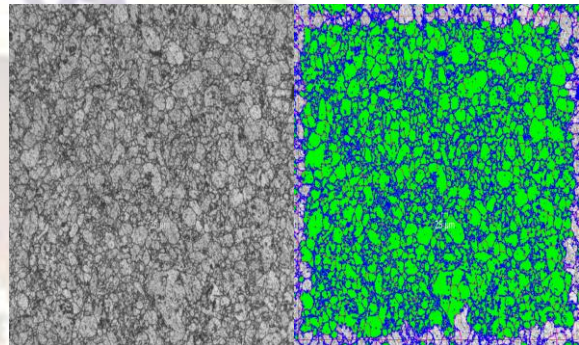**Figure.5a** Microstructure of 0.5% doped ZnO/Al composite

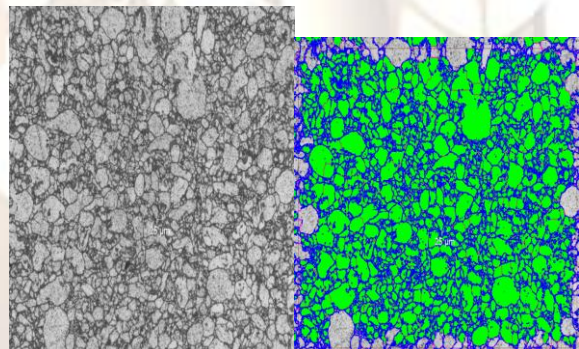**Figure.5b** Microstructure of 1% doped ZnO/Al composite

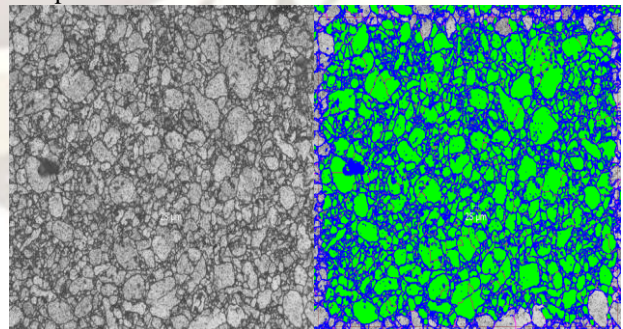**Figure.5c** Microstructure of 2.5% doped ZnO/Al composite

Figure.5d Microstructure of 5% doped ZnO/Al composite

3.5. Wear resistance test

The evaluation of wear resistance of the ZnO doped Aluminium samples are carried out on the basis of mass loss method and the results are

placed in Table1 and the corresponding graph is displayed in Fig.6. An incremental order was observed in reduction of wear loss from lower to higher wt % of nano-ZnO. However a relative steep drop from 6.0589 % wear loss at pure aluminum to 1.590 % wear loss at 1 wt% dopant is the maximum percentage reduction in wear loss. A further increase in nano-ZnO wt % has shown only a marginal reduction in wear value 1.590 % wear loss at 1 wt % to 1.300 % wear loss at 5 wt % nano-ZnO, which doesn't indicate much reduction in the wear value. This increase in wear resistance can be attributed to addition of ultra-fine ceramic reinforcement which possess high hardness, wear resistance and at the same time a strong interfacial bonding with the host matrix.

Table 1. Weight loss in samples after wear

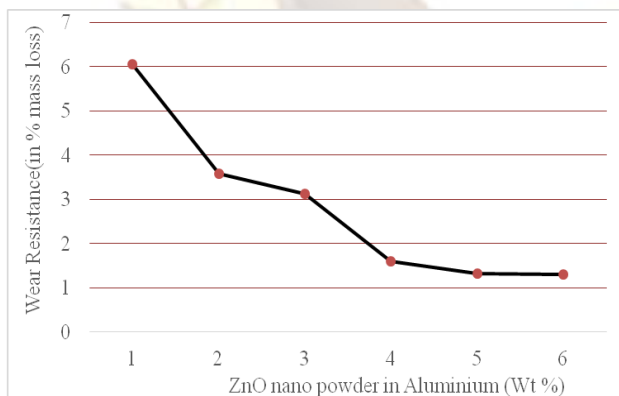| Wt% of ZnO doped Al Blocks	0 %	0.25 %	0.5 %	1 %	5 %
Initial Weight (gm)	4.9365	5.8713	4.4251	4.8852	5.3963
Final Weight (gm)	4.6374	5.6608	4.2872	4.8071	5.3261
Weight Loss (gm)	0.2991	0.2105	0.1379	0.0781	0.0702
Wear Resistance in % weight loss	6.0589	3.5852	3.1163	1.5987	1.3008

Figure.6 Variation of Wear Resistance with addition of nano-ZnO

3.6. Corrosion resistance test
The corrosion test on the nano-ZnO doped Aluminium specimens were conducted in two chemical baths; one containing NaCl and other with $MgSO_4$ standard solutions. The samples were tested for 50 hours in NaCl solution and 10 hours in $MgSO_4$ solution. In both the conditions the corrosive properties of the nano-ZnO doped Aluminium have been shown in Table2, Table3 and corresponding graphs are displayed in Fig.7, Fig.8. In NaCl solution, the pure Aluminium is having 1.0380 % of corrosion and by doping only 0.25 % the corrosion has scale down to 0.3488 %. At 0.5 wt % dopant corrosion drops to 0.2211% and 5% dopant the corrosion drops to 0.00127%. A sharp drop in corrosion value is observed by adding only a small wt % of nano-ZnO to Aluminium substrate.

This may be due to formation of an oxide layer due to quick reaction. Further drop in corrosion is almost proportion scale that can be as it is seen 0.2211 % corrosion value at 0.5% dopant to 0.00127 % of corrosion at 5% dopant can be tabulated as the corrosion resistance increases 10 times by increasing the dopant 10 times.

In $MgSO_4$, the corrosion resistance property of the nano-ZnO doped Aluminium increased at and above 0.5 wt% nano-ZnO dopant. Further the corrosion resistance property of the sample indicated the same trend as in the case of NaCl solution. It can be inferred from the result that a minimum of 0.5 wt% of nano-ZnO dopant is sufficient for the corrosion resistance when the environment contains $MgSO_4$.

Table 2. After corrosion of 50 hours with 3.5% NaCl solution

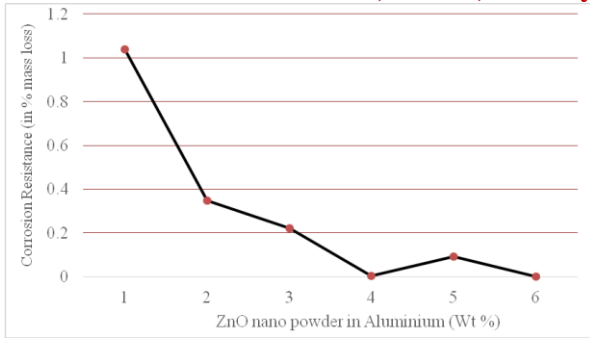| Wt% of ZnO doped Al blocks	Initial weight (gm)	Final weight (gm)	Weight loss (gm)	Corrosion Resistance (% weight loss)
0	23.7861	23.5392	0.2469	1.0380
0.25	24.9387	24.8517	0.0870	0.3488
0.5	23.6523	23.6000	0.0523	0.2211
1.0	23.9736	23.9725	0.0011	0.0045
2.5	24.4241	24.4012	0.0229	0.0937
5	23.5856	23.5853	0.0003	0.0012

Figure.7 Variation of Corrosion Resistance with addition of nano-ZnO after corrosion of 40 hours with 3.5% NaCl solution

Table 3 After corrosion of 10 hours with 0.5M MgSO₄ solution

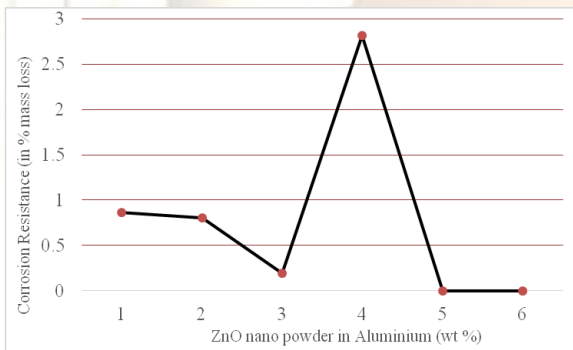| Wt% of ZnO doped Al Blocks	Initial weight (gm)	Final weight (gm)	Weight loss in gms	Corrosion Resistance in % weight loss
0	15.6381	15.5024	0.1357	0.8677
0.25	18.4753	18.3274	0.1479	0.8005
0.5	16.8293	16.7972	0.0321	0.1907
1.0	18.9412	18.408	0.5332	2.8150
2.5	15.3715	15.3713	0.0002	0.0013
5	17.4147	17.4146	0.0001	0.0005

Figure.8 Variation of Corrosion Resistance with addition of nano-ZnO after corrosion of 10 hours with 0.5M MgSO₄ solution

4. CONCLUSIONS

In the present work, ZnO nano powder is synthesized by a low temperature solution combustion method using zinc nitrate and sugar as fuel. The present research demonstrates improved microhardness and microstructure of ZnO nano powder reinforced Aluminium matrix as compared to pure Al matrix. Nano-ZnO crystals are well distributed in the Al matrix when doping percentage is increased up to 1 wt% as shown in SEM micrographs. Improved corrosion resistance and strength of ZnO nano powder reinforced Aluminium matrix can be attributed to densification of the matrix. Among all the samples that were evaluated, the optimum wt% of ZnO nano powder was found to be 1wt% with regard to uniform distribution of the reinforcement and highest micro hardness value for 1 wt % ZnO nano powder. Increasing trend in wear resistance of samples with increase in wt% of ZnO nano powder shows that ceramic particles as nano-reinforcement can impart superior wear resistance to the host aluminium matrix. Metal oxide nano particles are very efficient in imparting their inherent properties to the host matrix like high hardness and strength since they have high surface area to volume ratio.

REFERENCES
Journal Papers:
1. I. O Owate and E. Chukwuocha, Scientific Research and Essay. 3 (2007) 074-080.
2. A. I. Ogbonna, S. N. Asoegwu and P. C. Okebanama. Journal of Corrosion Science and Technology. 1 (2004) 135-146.
3. A. I. Onuchukwu, Journal of Corrosion Science and Technology. 2 (2004) 138-148.
4. K.S. Harishanand, Siddhant Datta, B.M. Nagabhushana, H. Nagabhushana, M.M. Benal, International Journal of Engineering Research and Applications, 5 (2012) 1030-1035.
5. A. Ansary Yar, M. Montazerian, H. Abdizadeh, H.R. Baharvandi. Journal of Alloys and Compounds 484 (2009) 400–404.
6. Chunyan Tiana, Ning Liua, Maohua Lua. Journal of materials processing technology 205 (2 008) 411-418.
7. Wang Qian. Trans. Nonferrous. Soc. China 17 (2007) 622-625.
8. Abdulkadir EKSI, Suleyman SARITAS Turkish. J. Eng. Env. Sci. 26 (2002) 377 - 384.
9. B. Weintraub, Z. Zhou, Y. Li, and Y. Deng, Nanoscale, 2 (2010) 1573–1587.
10. Y. Xia, P. Yang, Y. Sun et al., Advanced Materials, 15 (2003) 353–389.
11. G. C. Yi, C. Wang, and W. I. Park, Semiconductor Science and Technology, 20 (2005) 22–34.
12. Z. L. Wang, Chinese Science Bulletin, 54 (2009) 4021–4034.
13. F. Lu, W. Cai, and Y. Zhang. Advanced Functional Materials, 18 (2008) 1047–1056.
14. L. Zhang, Y. Ding, M. Povey, D. York, Prog. Nat. Sci. 18 (2008) 939–944.
15. J. Xie, H. Deng, Z.Q. Xu, Y. Li, J. Huang, J. Cryst. Growth 292 (2006) 227–229.
16. C. Liewhiran, S. Phanichphant, Sensors 7 (2007) 650–675.

17.   A. Sasaki, W. Hara, A. Mastuda, N. Tateda, K. Saitom, M. Yoshimoto, Appl. Phys. Lett. 86 (2005) 231911–231921.

18.   M.K. Patra, K. Manzoor, M. Manoth, S.R. Vadera, N. Kumar, J. Lumin. 128 (2008) 267–272.

19.   L. Vayssieres, Adv. Mater. 15 (2003) 464–466.

20.   J.J. Kingsley, K.C. Patil, Mater. Lett. 6 (1988) 427–432.

21.   B.M. Nagabhushana, R.P.S. Chakradhar, K.P. Ramesh, .T. Chandrappa, Phil. Mag. 90 (2010) 2009–2025.

22.   S. Ekambaram, N. Arul Dhas, K.C. Patil, Int. J. Self-prop. High-temp. Synth. 4 (1995) 85–93.

23.   G.K. Willamson, W.H. Hall, Acta Metall. 1 (1953) 22–31.

24.   J. Rodrigueg-carvajal, Fullprof. 2000: a program for Rietveld, profile matching and integrated intensity refinements for X-ray and neutron data. Version 1.6. Laboratorie Leon, Brillounin, Gifsuryvette, France, 2009.

25.   A. Kajbafvala, M.R. Shayegh, M. Mazloumi, S. Zanganeh, S.K. Aidin Lak, Sadrnezhaad, J. Alloys Compd. 469 (2009) 293–297.

26.   M. Ristic, S. Musiˇıc, M. Ivanda, S. Popoviˇıc, J. Alloys Compd. 397 (2005) L1–L4.

27.   A. Fonoberov, A.A. Balandin, Phys. Rev. B 70 (2004) 233205–233208.

28.   K.A. Alim, V.A. Fonoberov, M. Shamsa, A.A. Balandina, J. Appl. Phys. 97 (2005) 124313–124323.

29.   A. Jagannatha Reddy, M.K. Kokila, H. Nagabhushana, J.L. Rao, C. Shivakumara B.M. Nagabhushana, R.P.S. Chakradhar. Spectrochimica Acta Part A 81 (2011) 53-58.